

Bayesian Discovery of Threat Networks

Steven Thomas Smith, *Senior Member, IEEE*, Edward K. Kao, *Member, IEEE*,
Kenneth D. Senne, *Life Fellow, IEEE*, Garrett Bernstein, and Scott Philips

Abstract—A novel unified Bayesian framework for network detection is developed, under which a detection algorithm is derived based on random walks on graphs. The algorithm detects threat networks using partial observations of their activity, and is proved to be optimum in the Neyman-Pearson sense. The algorithm is defined by a graph, at least one observation, and a diffusion model for threat. A link to well-known spectral detection methods is provided, and the equivalence of the random walk and harmonic solutions to the Bayesian formulation is proven. A general diffusion model is introduced that utilizes spatio-temporal relationships between vertices, and is used for a specific space-time formulation that leads to significant performance improvements on coordinated covert networks. This performance is demonstrated using a new hybrid mixed-membership blockmodel introduced to simulate random covert networks with realistic properties.

Index Terms—Network detection, optimal detection, maximum likelihood detection, community detection, network theory (graphs), graph theory, diffusion on graphs, random walks on graphs, dynamic network models, Bayesian methods, harmonic analysis, eigenvector centrality, Laplace equations.

I. INTRODUCTION

NETWORK detection is the objective in many diverse graph analytic applications, ranging from graph partitioning, mesh segmentation, manifold learning, community detection [44], network anomaly detection [10], [30], and the discovery of clandestine networks [32], [43], [52], [56], [70]. A new Bayesian approach to network detection is developed and analyzed in this paper, with specific application to detecting small, covert networks embedded within much larger background networks. The novel approach is based on a Bayesian probabilistic framework where the probability of threat is derived from an observation model and an a priori threat diffusion model. Specifically, observed threats from one or more vertices are propagated through the graph using a

model based on random walks represented as Markov chains with absorbing states. The resulting network detection algorithm is proved to be optimum in the Neyman-Pearson sense of maximizing the probability of detection at a fixed false alarm probability. In the specific case of space-time graphs with time-stamped edges, a model for threat diffusion yields the new space-time threat propagation algorithm, which is shown to be an optimal detector for covert networks with coordinated activity.

Network detectors are analyzed using both a stochastic framework of random walks on the graph and a probabilistic framework. The two frameworks are shown to be equivalent, providing an original, unified approach for Bayesian network detection. Performance for a variety of Bayesian network detection algorithms is shown with both a stochastic blockmodel and a new hybrid mixed-membership blockmodel (HMMB) introduced to simulate random covert networks with realistic properties.

Using insights from algebraic graph theory, the connection between this unified framework and other spectral-based network detection methods [18], [22], [44] is shown, and the two approaches are contrasted by comparing their different optimality criteria based on detection probability and subgraph connectivity properties. The random walk framework provides a connection with many other well-known graph analytic methods that may also be posed in this context [7], [11], [15], [34], [46], [54], [62]. In contrast to other research on network detection, rather than using a sensor network to detect signals [3], [13], [30], the signal of interest in this paper is the network. In this sense the paper is also related to work on so-called manifold learning methods [8], [10], [16], although the network to be detected is a subgraph of an existing network, and therefore the methods described here belong to a class of network anomaly detection [10] as well as maximum-likelihood methods for network detection [21].

Threat network discovery is predicated on the existence of observations of network relationships. Detection of network communities is most likely to be effective if the communities exhibit high levels of connection activity. The covert networks of interest in this paper exist to accomplish nefarious, illegal, or terrorism goals, while “hiding in plain sight” [70]. Covert networks necessarily adopt operational procedures to remain hidden and robustly adapt to losses of parts of the network [9], [52], [61], [66].

This paper’s major contributions are organized into a description of the novel approach to Bayesian network detection in Section III, and showing and comparing detection performance using simulations of realistic networks in Section IV.

Manuscript received November 15, 2013; revised March 17, 2014; accepted May 29, 2014. Date of publication July 08, 2014; date of current version September 8, 2014. The associate editor coordinating the review of this manuscript and approving it for publication was Prof. Francesco Verde. This work is sponsored by the Assistant Secretary of Defense for Research & Engineering under Air Force Contract FA8721-05-C-0002. Opinions, interpretations, conclusions and recommendations are those of the author and are not necessarily endorsed by the United States Government.

S. T. Smith, K. D. Senne, G. Bernstein, and S. Philips are with the MIT Lincoln Laboratory, Lexington, MA 02420 USA (e-mail: stsmith@ll.mit.edu; edward.kao@ll.mit.edu; senne@ll.mit.edu; garrett.bernstein@ll.mit.edu).

E. K. Kao is with the MIT Lincoln Laboratory, Lexington, MA 02420 USA, and also with the Department of Statistics, Harvard University; Cambridge MA USA 02138 (e-mail: edwardkao@fas.harvard.edu).

Color versions of one or more of the figures in this paper are available online at <http://ieeexplore.ieee.org>.

Digital Object Identifier 10.1109/TSP.2014.2336613

Fundamental new results are established in Theorems 1–3, which prove a maximum principal for threat propagation, provide a nonnegative basis for the principal invariant subspace, and prove the equivalence between the probabilistic and stochastic realization approaches of threat propagation. The Neyman–Pearson optimality of threat propagation is established in Theorem 4.

II. BACKGROUND

A. Notation

A graph $G = (V, E)$ is defined by two sets, the vertices V , and the edges $E \subset [V]^2$, in which $[V]^2$ denotes the set of 2-element subsets of V [17]. For example, the sets $V = \{1, 2, 3\}$, $E = \{\{1, 2\}, \{2, 3\}\}$ describe a simple graph with undirected edges between vertices 1 and 2, and 2 and 3: $\textcircled{1} - \textcircled{2} - \textcircled{3}$. The *order* and *size* of G are defined to be $\#V$ and $\#E$, respectively. A *subgraph* $G' \subseteq G$ is a graph (V', E') with $V' \subseteq V$ and $E' \subseteq E$. If E' contains all edges in E with both endpoints in V' , then $G' = G[V']$ is the *induced subgraph* of V' . The *adjacency matrix* $\mathbf{A} = \mathbf{A}(G)$ of G is the $\{0, 1\}$ -matrix with $a_{ij} = 1$ iff $\{i, j\} \in E$. In the example, $\mathbf{A} = \begin{pmatrix} 0 & 1 & 0 \\ 1 & 0 & 1 \\ 0 & 1 & 0 \end{pmatrix}$. The adjacency matrix of simple or undirected graphs is necessarily symmetric. The *degree matrix* $\mathbf{D} = \text{Diag}(\mathbf{A} \cdot \mathbf{1})$ is the diagonal matrix of the vector of degrees of all vertices, where $\mathbf{1} = (1, \dots, 1)^T$ is the vector of all ones. The *neighborhood* $N(u) = \{v : \{u, v\} \in E\}$ of a vertex $u \in V$ is the set of vertices adjacent to u , or equivalently, the set of nonzero elements in the u -th row of \mathbf{A} . The *vertex space* $\mathcal{V}(G)$ of G is the vector space of functions $f: V \rightarrow \{0, 1\}$.

A *directed graph* G_σ is defined by an orientation map $\sigma: [V]^2 \rightarrow V \times V$ (the ordered Cartesian product of V with itself) in which the first and second coordinates are called the initial and terminal vertices, respectively. A *strongly connected graph* is a connected graph for which a directed path exists between any two vertices. The *incidence matrix* $\mathbf{B} = \mathbf{B}(G_\sigma)$ of G_σ is the $(0, \pm 1)$ -matrix of size $\#V$ -by- $\#E$ with $\mathbf{B}_{ie} = \pm 1$, if i is an terminal/initial vertex of $\sigma(e)$, and 0 otherwise. For example, the directed graph $\textcircled{1} \times \textcircled{2} \rightarrow \textcircled{3}$ has incidence matrix $\mathbf{B} = \begin{pmatrix} 1 & 0 \\ -1 & -1 \\ 0 & 1 \end{pmatrix}$. The *unnormalized Laplacian matrix* or *Kirchhoff matrix* \mathbf{Q} of a graph, the (normalized) *Laplacian matrix* \mathbf{L} , and the *generalized or asymmetric Laplacian matrix* \mathbf{L} are, respectively,

$$\mathbf{Q} = \mathbf{B}\mathbf{B}^T = \mathbf{D} - \mathbf{A}, \quad (1)$$

$$\mathbf{L} = \mathbf{D}^{-1/2}\mathbf{Q}\mathbf{D}^{-1/2} = \mathbf{I} - \mathbf{D}^{-1/2}\mathbf{A}\mathbf{D}^{-1/2}, \quad (2)$$

$$\mathbf{L} = \mathbf{D}^{-1/2}\mathbf{L}\mathbf{D}^{1/2} = \mathbf{D}^{-1}\mathbf{Q} = \mathbf{I} - \mathbf{D}^{-1}\mathbf{A}. \quad (3)$$

In the example, \mathbf{L} is immediately recognized as a discretization of the second derivative $-d^2/dx^2$, i.e. the negative of the 1-d Laplacian operator $\Delta = \partial^2/\partial x^2 + \partial^2/\partial y^2 + \dots$ that appears in physical applications. The connection between the Laplacian matrices and physical applications is made through Green’s first identity, a link that explains many theoretical and performance advantages of the normalized Laplacian over the Kirchhoff matrix across applications [14], [64], [67], [68].

Solutions to Laplace’s equation on a graph are directly connected to random walks or discrete Markov chains on the vertices of the graph, which provide stochastic realizations for harmonic problems. A (*right*) *stochastic matrix* \mathbf{T} of a graph is a nonnegative matrix such that $\mathbf{T}\mathbf{1} = \mathbf{1}$. This represents a state transition matrix of a random walk on the graph with transition probability t_{ij} of jumping from vertex v_i to vertex v_j . The Perron–Frobenius theorem guarantees if \mathbf{T} is irreducible (i.e. G is strongly connected) then there exists a stationary probability distribution \mathbf{p}_v on V such that $\mathbf{p}^T\mathbf{T} = \mathbf{p}^T$ [26], [28]. Random walk realizations can be used to describe the solution to harmonic boundary value problems, e.g. equilibrium thermodynamics [47], [51], in which given values are proscribed at specific “boundary” vertices.

B. Network Detection

Network detection is a special class of the more general graph partitioning (GP) problem in which the binary decision of membership or non-membership for each graph vertex must be determined. Indeed, the network detection problem for a graph G of order N results in a 2^N -ary multiple hypothesis test over the vertex space $\mathcal{V}(G)$, and, when detection optimality is considered, an optimal test involves partitioning the measurement space into 2^N regions yielding a maximum probability of detection (PD). This NP-hard combinatoric problem is computationally and analytically intractable. In general, network detection methods invoke various relaxation approaches to avoid the NP-hard network detection problem. The new Bayesian threat propagation approach taken in this paper is to greatly simplify the general 2^N -ary multiple hypothesis test by applying the random walk model and treating it as N independent binary hypothesis tests. This approach is related to existing network detection methods by posing an optimization problem on the graph—e.g. threat propagation maximizes PD—and through solutions to Laplace’s equation on graphs. Because many network detection algorithms involve such solutions, a key fact is that the constant vector $\mathbf{1} = (1, \dots, 1)^T$ is in the kernel of the Laplacian,

$$\mathbf{Q}\mathbf{1} = \mathbf{0}; \quad \mathbf{L}\mathbf{1} = \mathbf{0}. \quad (4)$$

This constant solution does not distinguish between vertices at all, a deficiency that may be resolved in a variety of ways.

Efficient graph partitioning algorithms and analysis appeared in the 1970s with Donath and Hoffman’s eigenvalue-based bounds for graph partitioning [18] and Fiedler’s connectivity analysis and graph partitioning algorithm [22] which established the connection between a graph’s algebraic properties and the spectrum of its Kirchhoff Laplacian matrix $\mathbf{Q} = \mathbf{D} - \mathbf{A}$ [Eq. (1)]. Spectral methods solve the graph partitioning problem by optimizing various subgraph connectivity properties. Similarly, the threat propagation algorithm developed here in Section III optimizes the probability of detecting a subgraph for a specific Bayesian model. Though the optimality criteria for spectral methods and threat propagation are different, all these network detection methods must address the fundamental problem of avoiding the trivial solution of constant harmonic functions on graphs. Threat

propagation avoids this problem by using observation vertices and a priori probability of threat diffusion (Section III-A). Spectral methods take a complementary approach to avoid this problem by using an alternate optimization criterion that depends upon the network's topology.

The *cut size* of a subgraph—the number of edges necessary to remove to separate the subgraph from the graph—is quantified by the quadratic form $\mathbf{s}^T \mathbf{Q} \mathbf{s}$, where $\mathbf{s} = (\pm 1, \dots, \pm 1)^T$ is a ± 1 -vector whose entries are determined by subgraph membership [50]. Minimizing this quadratic form over \mathbf{s} , whose solution is an eigenvalue problem for the graph Laplacian, provides a network detection algorithm based on the model of minimal cut size. However, there is a paradox in the application of spectral methods to network detection: the smallest eigenvalue of the graph Laplacian $\lambda_0(\mathbf{Q}) = 0$ corresponds to the eigenvector $\mathbf{1}$ constant over all vertices, which fails to discriminate between subgraphs. Intuitively this degenerate constant solution makes sense because the two subgraphs with minimal (zero) subgraph cut size are the entire graph itself ($\mathbf{s} \equiv \mathbf{1}$), or the null graph ($\mathbf{s} \equiv -\mathbf{1}$). This property manifests itself in many well-known results from complex analysis, such as the maximum principle.

Fiedler showed that if rather the eigenvector ξ_1 corresponding to the second smallest eigenvalue $\lambda_1(\mathbf{Q})$ of \mathbf{Q} is used (many authors write $\lambda_1 = 0$ and λ_2 rather than the zero offset indexing $\lambda_0 = 0$ and λ_1 used here), then for every nonpositive constant $c \leq 0$, the subgraph whose vertices are defined by the threshold $\xi_1 \geq c$ is necessarily connected. This algorithm is called *spectral detection*. Given a graph G , the number $\lambda_1(\mathbf{Q})$ is called the *Fiedler value* of G , and the corresponding eigenvector $\xi_1(\mathbf{Q})$ is called the *Fiedler vector*. Completely analogous with comparison theorems in Riemannian geometry that relate topological properties of manifolds to algebraic properties of the Laplacian, many graph topological properties are tied to its Laplacian. For example, the graph's diameter D and the minimum degree d_{\min} provide lower and upper bounds for the Fiedler value $\lambda_1(\mathbf{Q})$: $4/(nD) \leq \lambda_1(\mathbf{Q}) \leq n/(n-1) \cdot d_{\min}$ [41]. This inequality explains why the Fiedler value is also called the *algebraic connectivity*: the greater the Fiedler value, the smaller the graph diameter, implying greater graph connectivity. If the normalized Laplacian \mathbf{L} of Eq. (2) is used, the corresponding inequality involving the generalized eigenvalue $\lambda_1(\mathbf{L}) = \lambda_1(\mathbf{Q}, \mathbf{D})$ involves the graph's diameter D and volume V : $1/(DV) \leq \lambda_1(\mathbf{L}) \leq n/(n-1)$ [14].

Because in practice spectral detection with its implicit assumption of minimizing the cut size oftentimes does not detect intuitively appealing subgraphs, Newman introduced the alternate criterion of subgraph “modularity” for subgraph detection [44]. Rather than minimize the cut size, Newman proposes to maximize the subgraph connectivity relative to background graph connectivity, which yields the quadratic maximization problem $\max_{\mathbf{s}} \mathbf{s}^T \mathbf{M} \mathbf{s}$, where $\mathbf{M} = \mathbf{A} - V^{-1} \mathbf{d} \mathbf{d}^T$ is Newman's *modularity matrix*, \mathbf{A} is the adjacency matrix, $(\mathbf{d})_i = d_i$ is the degree vector, and $V = \mathbf{1}^T \mathbf{d}$ is the graph volume [44]. Newman's modularity-based graph partitioning algorithm, also called community detection, involves thresholding the values of the principal eigenvector of \mathbf{M} . Miller et al. [38]–[40] also consider thresholding arbitrary eigenvectors of the modularity

matrix, which by the Courant minimax principle biases the Newman community detection algorithm to smaller subgraphs, a desirable property for many applications. They also outline an approach for exploiting observations within the spectral framework [38].

Other graph partitioning methods invoke alternate relaxation approaches that yield practical detection/partitioning algorithms such as semidefinite programming (SDP) [6], [35], [69]. A class of graph partitioning algorithms is based on infinite random walks on graphs [59]. Zhou and Lipowsky define proximity using the average distance between vertices [72]. Anderson et al. define a local version biased towards specific vertices [4]. Mahoney et al. develop a local spectral partitioning method by augmenting the quadratic optimization problem with a locality constraint and relaxing to a convex SDP [37]. An important dual to network detection is the problem of identifying the source of an epidemic or rumor using observations on the graph [53], [54]. Another related problem is the determination of graph topologies for which epidemic spreading occurs [11], [62]. The approach adopted in this paper has fundamentally different objectives and propagation models than the closely-related epidemiological problems. These problems focus on disease spreading to large portions of the entire graph, which arises because disease may spread from any infected neighbor—yielding a logical OR of neighborhood disease. Network detection focuses on discovering a subgraph most likely associated with a set of observed vertices, assuming random walk propagation to the observations—yielding an arithmetic mean of neighborhood threat. All of these methods are related to spectral partitioning through the graph Laplacian.

III. BAYESIAN NETWORK DETECTION

The Bayesian model developed here depends upon threat observation and propagation via random walks over both space and time, and the underlying probabilistic models that govern inference from observation to threat, then propagation of threat throughout the graph. Bayes' rule is used to develop a network detection approach for spatial-only, space-time, and hybrid graphs. The framework assumes a given Markov chain model for transition probabilities, and hence knowledge of the graph, and a diffusion model for threat. Neyman–Pearson optimality is developed in the context of network detection with a simple binary hypothesis, and it is proved that threat propagation is optimum in this sense.

The framework is sufficiently general to capture graphs formed by many possible relationships between entities, from simple graphs with vertices that represent a single type of entity, to bipartite or multipartite graphs with heterogeneous entities. For example, an email network is a bipartite graph comprised of two types of vertices: individual people and individual email messages, with edges representing a connection between people and messages. Without loss of generality, all entity types to be detected are represented as vertices in the graph, and their connections are represented by edges weighted by scalar transition probabilities.

Network detection is the problem of identifying a specific subgraph within a given graph $G = (V, E)$. Assume that

within G , a foreground or “threat” network V^Θ exists defined by an (unknown) binary random variable:

Definition 1 Threat is a $\{0, 1\}$ -valued discrete random variable. Threat on a graph $G = (V, E)$ is a $\{0, 1\}$ -valued function $\Theta \in \mathcal{V}(G)$. Threat at the vertex v is denoted Θ_v . A vertex $v \in V$ is in the foreground if $\Theta_v = 1$, otherwise v is in the background.

The foreground or threat vertices are the set $V^\Theta = \{v : \Theta_v = 1\}$, and the foreground or threat network is the induced subgraph $G^\Theta = G[V^\Theta]$. A network detector of the subgraph G^Θ is a collection of binary hypothesis tests to decide which of the graph’s vertices belong to the foreground vertices V^Θ . Formally, a network detector is an element of the vertex space of G :

Definition 2 Let $G = (V, E)$ be a graph. A network detector ϕ on G is a $\{0, 1\}$ -valued function $\phi \in \mathcal{V}(G)$. The induced subgraph $G^\phi = G[V^\phi]$ of $V^\phi = \{v : \phi_v = 1\}$ is called the foreground network and the induced subgraph $G^{\bar{\phi}} = G[V^{\bar{\phi}}]$ of $V^{\bar{\phi}} = \{v : \phi_v = 0\}$ is called the background network, in which $\bar{\phi}$ denotes the logical complement of ϕ .

The correlation between a network detector ϕ and the actual threat network defined by the function Θ determines the detection performance of ϕ , measured using the detector’s probability of detection (PD) and probability of false alarm (PFA). The PD and PFA of ϕ are the fraction of correct and incorrect foreground vertices determined by ϕ :

$$\text{PD}^\phi = \#(V^\phi \cap V^\Theta) / \#V^\Theta, \quad (5)$$

$$\text{PFA}^\phi = \#(V^\phi \cap V^{\bar{\Theta}}) / \#V^{\bar{\Theta}}. \quad (6)$$

Observation models are now introduced and applied in the sequel to threat propagation models in the contexts of spatial-only graphs, space-time graphs whose edges have time stamps, and finally a hybrid graphs with edges of mixed type. Assume that there are C observed vertices $\{v_{b_1}, \dots, v_{b_C}\} \subset V$ at which observations are taken. In the resulting Laplacian problem, these are “boundary” vertices, and the rest are “interior.” The simplest case involves scalar measurements; however, there is a straightforward extension to multidimensional observations.

Definition 3 Let $G = (V, E)$ be a graph. An observation on the graph is a vector $\mathbf{z}: \{v_{b_1}, \dots, v_{b_C}\} \rightarrow M \subset \mathbb{R}^C$ from C vertices to a measurement space $M \subset \mathbb{R}^C$.

Ideally, observation of a foreground and/or background vertices unequivocally determines whether the observed vertices lie in the foreground or background networks, i.e. given a foreground graph $G^\Theta = G[V^\Theta]$ and a foreground vertex $v \in V^\Theta$, an observation vector \mathbf{z} evaluated at v would yield $\mathbf{z}(v) = 1$, and \mathbf{z} evaluated at a background vertex $v' \in V^{\bar{\Theta}}$ would yield $\mathbf{z}(v') = 0$. In general, it is assumed that the observation $\mathbf{z}(v)$ at v and the threat Θ_v at v are not statistically independent, i.e. $f(\mathbf{z}(v) | \Theta_v) \neq f(\mathbf{z}(v))$ for probability density f , so that there is positive mutual information between

$\mathbf{z}(v)$ and Θ_v . Bayes’ rule for determining how likely a vertex is to be a foreground member or not depends on the model linking observations to threat:

Definition 4 Let $G^\Theta = G[V^\Theta]$ be the foreground graph of a graph G determined by $\Theta \in \mathcal{V}(G)$, and let $\mathbf{z}: \{v_{b_1}, \dots, v_{b_C}\} \rightarrow M \subset \mathbb{R}^C$ be an observation on G . The conditional probability density $f(\mathbf{z}(v) | \Theta_v)$ is called the observation model of vertex $v \in V$.

The simplest, ideal observation model equates threat with observation so that $f_{\text{ideal}}(\mathbf{z}(v) | \Theta_v) = \delta_{\mathbf{z}(v)\Theta_v}$ in which δ_{ij} is the Kronecker delta. Though the threat network hypotheses are being treated here independently at each vertex, this framework allows for more sophisticated global models that include hypotheses over two or more vertices.

The remainder of this section is devoted to the development of Bayesian methods of using measurements on a graph to determine the probability of threat on a graph in various contexts—spatial-only, space-timed, and the hybrid case—then showing that these methods are optimum in the Neyman–Pearson sense of maximizing the probability of detection at a given false alarm rate. The motivating problem is:

Problem 1 Detect the foreground graph $G^\Theta = G[V^\Theta]$ in the graph $G = (V, E)$ with an unknown foreground $\Theta \in \mathcal{V}(G)$ and known observation vector $\mathbf{z}(v_{b_1}, \dots, v_{b_C})$.

This problem is addressed by computing the probability of threat $P(\Theta_v)$ at all graph vertices from the measurements at observed vertices using an observation model and the application of Bayes’ rule.

A. Spatial Threat Propagation

A spatial threat propagation algorithm is motivated and developed now, which will be used in the subsequent space-time generalization, and will demonstrate the connection to spectral network detection methods. A vertex is declared to be threatening if the observed threat propagates to that vertex. We wish to compute the probability of threat $P(\Theta_v = 1 | \mathbf{z})$ at all vertices $v \in V$ in a graph $G = (V, E)$ given an observation $\mathbf{z}(v_{b_1}, \dots, v_{b_C})$ on G . Implicit in Problem 1 is a coordinated threat network in which threat propagates via network connections, i.e. graph edges. For simplicity, probabilities conditioned on the observation \mathbf{z} will be written

$$\theta_v = P(\Theta_v | \mathbf{z}) \quad (7)$$

with an implied dependence on the observation vector \mathbf{z} and the event $\Theta_v = 1$ expressed as Θ_v .

To model the diffusion of threat throughout the graph, we introduce an a priori probability ψ_v at each vertex v that represents threat diffusion at v . ψ_v is the probability that threat propagates through vertex v to its neighbors, otherwise threat propagates to an absorbing “non-threat” state with probability $1 - \psi_v$. A threat diffusion event at v is represented by the $\{0, 1\}$ -valued r.v. Ψ_v :

Definition 5 The threat diffusion model of a graph $G = (V, E)$ with observation \mathbf{z} is given by the a priori $\{0, 1\}$ -valued event Ψ_v that threat Θ_v propagates through v with probability ψ_v .

Threat propagation on the graph from the observed vertices to all other vertices is defined as an average over all random walks between vertices and the observations. A single random walk between v and an observed vertex v_{b_c} is defined by the sequence

$$\text{walk}_{v \rightarrow v_{b_c}} = (v_{w_1}, v_{w_2}, \dots, v_{w_L}) \quad (8)$$

with endpoints $v_{w_1} = v$ and $v_{w_L} = v_{b_c}$, comprised of L steps along vertices $v_{w_l} \in V$. The probabilities for each step of the random walk are defined by the elements of the transition matrix t_{vu} from vertex v to u , multiplied by the a priori probability ψ_v that threat propagates through v . The assumption that G is strongly connected guarantees the existence of a walk between every vertex and every observation. Threat may be absorbed to the non-threat state with probability $1 - \psi_{v_{w_l}}$ at each step. The simplest models for both the transition and a priori probabilities are uniform: $t_{ij} = 1/\text{degree}(v_i)$ for $(i, j) \in E$, i.e. $\mathbf{T} = \mathbf{D}^{-1}\mathbf{A}$, and $\psi_v \equiv 1$. The implications of these simple models as well as more general weighted models will be explored throughout this section.

The indicator function

$$I_{\text{walk}_{v \rightarrow v_{b_c}}} = \prod_{l=1}^L \Psi_{v_{w_l}} \quad (9)$$

determines whether threat propagates along the walk or is absorbed into the non-threat state (the superscript ' l ' allows for the possibility of repeated vertices in the sequence). The definition of threat propagation is captured in three parts: (1) a single random walk, $\text{walk}_{v \rightarrow v_{b_c}}$, with $I_{\text{walk}_{v \rightarrow v_{b_c}}} = 1$ yields threat probability $\theta_{v_{b_c}}$ at v ; (2) the probability of threat averaged over all such random walks; (3) the random variable obtained by averaging the r.v. $\Theta_{v_{b_c}}$ over all such random walks. Formally,

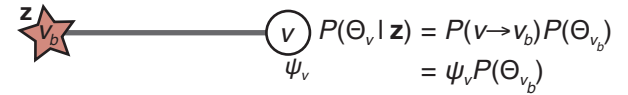
Definition 6 (Threat Propagation). Let $G = (V, E)$ be a strongly connected graph with threat probabilities $\theta_{v_{b_1}}, \dots, \theta_{v_{b_C}}$ at observed vertices v_{b_1}, \dots, v_{b_C} and the threat diffusion model ψ_v for all $v \in V$. (1) For a random walk on G from v to observed vertex v_{b_c} with transition matrix \mathbf{T} , $\text{walk}_{v \rightarrow v_{b_c}} = (v_{w_1}, v_{w_2}, \dots, v_{w_L})$, if events $\Psi_{v_{w_l}} \equiv 1$ for all vertices v_{w_l} along the walk, then the threat propagation from v_{b_c} to v along $\text{walk}_{v \rightarrow v_{b_c}}$ is defined to be $\theta_{v_{b_c}}$; otherwise, the threat equals zero. (2) Threat propagation to vertex v is defined as the expectation of threat propagation to v along all random walks emanating from v ,

$$\theta_v = \lim_{K \rightarrow \infty} \frac{1}{K} \sum_k I_{\text{walk}_{v \rightarrow v_{b_c}(k)}} \theta_{v_{b_c}(k)}, \quad (10)$$

where the k th walk terminates at the observed vertex $v_{b_c(k)}$. (3) Random threat propagation to vertex v is defined as the random variable

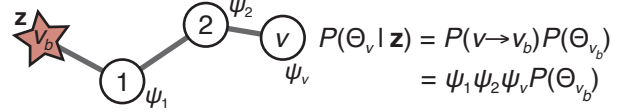
$$\bar{\Theta}_v = \lim_{K \rightarrow \infty} \frac{1}{K} \sum_k I_{\text{walk}_{v \rightarrow v_{b_c}(k)}} \Theta_{v_{b_c}(k)} \quad (11)$$

Single hop walk



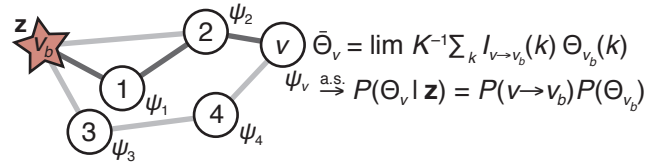
$$P(\Theta_v | \mathbf{z}) = P(v \rightarrow v_b) P(\Theta_{v_b}) = \psi_v P(\Theta_{v_b})$$

Multiple hop walk



$$P(\Theta_v | \mathbf{z}) = P(v \rightarrow v_b) P(\Theta_{v_b}) = \psi_1 \psi_2 \psi_v P(\Theta_{v_b})$$

Random walk



$$\bar{\Theta}_v = \lim_{K \rightarrow \infty} K^{-1} \sum_k I_{v \rightarrow v_b}(k) \Theta_{v_b}(k)$$

$$\psi_v \xrightarrow{\text{a.s.}} P(\Theta_v | \mathbf{z}) = P(v \rightarrow v_b) P(\Theta_{v_b})$$

Fig. 1. Illustration of the random walk representation for threat propagation from Definition 6 and Eqs. (11) and (33), for the case of a single observation. The upper illustration shows the simplest, trivial case with a single hop from the observation to the vertex. The middle illustration shows the next simplest case with multiple hops. The lower illustration shows an example of the general case, comprised of the simpler multiple hop case.

with independent draws $\Theta_{v_{b_c}(k)}^{(k)}$ of the observed threat.

Fig. 1 illustrates threat propagation of Definition 6 and Eq. (11) [and Eq. (33) from the sequel] for the simple-to-general cases of a single hop, multiple hops, and an arbitrary random walk. By the law of large numbers,

$$\bar{\Theta}_v \xrightarrow{\text{a.s.}} \theta_v \quad \text{as } K \rightarrow \infty. \quad (12)$$

The random walk model is described using the distinct yet equivalent probabilistic and stochastic realization representations. The probabilistic representation describes the threat probabilities by a Laplacian system of linear equations, which amounts to equating threat at a vertex to an average of neighboring probabilities. In contrast, the stochastic realization representation presented below in Section III-A2 describes the evolution of a single random walk realization whose ensemble statistics are described by the probabilistic representation, presented next.

1) *Probabilistic Approach:* Consider the (unobserved) vertex $v \notin \{v_{b_1}, \dots, v_{b_C}\}$ with neighbors $N(v) = \{v_{n_1}, \dots, v_{n_{d_v}}\} \subset V$ and $d_v = \text{degree}(v)$. The probabilistic equation for threat propagation from the neighbors of a vertex v follows immediately from Definition 6 from first-step analysis, yielding the *threat propagation equation*:

$$\theta_v = \psi_v \sum_{u \in N(v)} t_{vu} \theta_u, \quad (13)$$

which is simply the average of the neighboring threat probabilities weighted by transition probabilities $t_{vu} = (\mathbf{T})_{vu}$. Note that because $\mathbf{A}\theta \geq \theta$, θ_v is a subharmonic function on the graph [19], [28]. In the simplest case of uniform transition probabilities, $\mathbf{T} = \mathbf{D}^{-1}\mathbf{A}$ and

$$\theta_v = \frac{\psi_v}{d_v} \sum_{u \in N(v)} \theta_u. \quad (14)$$

Expressed in matrix-vector notation, Eqs. (13) and (14) become

$$\boldsymbol{\theta} = \boldsymbol{\Psi} \mathbf{T} \boldsymbol{\theta} \quad \text{and} \quad \boldsymbol{\theta} = \boldsymbol{\Psi} \mathbf{D}^{-1} \mathbf{A} \boldsymbol{\theta}, \quad (15)$$

where $(\boldsymbol{\theta})_v = \theta_v$, $\boldsymbol{\Psi} = \text{Diag}(\psi_v)$ is the diagonal matrix of a priori threat diffusion probabilities, \mathbf{T} , \mathbf{D} , and \mathbf{A} are, respectively, the transition, degree, and adjacency matrices. The threat probabilities at the observed vertices v_{b_1}, \dots, v_{b_C} are determined by the observation model of Definition 4, and threat probabilities at all other vertices are determined by solving Eq. (15), as with all Laplacian boundary value problems.

As seen in the spectral network detection methods in Section II-B, many network detection algorithms exploit properties of the graph Laplacian, and therefore must address the fundamental challenge posed by the implication of the maximum principle that harmonic functions are constant [19] in many important situations [Eq. (4)], and because the constant function does not distinguish between vertices, detection algorithms that rely only on solutions to Laplace's equation provide a futile approach to detection. If the boundary is constant, i.e. the probability of threat on all observed vertices is equal, then this is the probability of threat on every vertex in the graph. The later example is relevant in the practical case in which there a single observation. The maximum principle applies directly to threat propagation with uniform prior $\boldsymbol{\Psi} = \mathbf{I}$ and uniform probability of threat p_o on the observed vertices: Eqs. (15) are recognized as Laplace's equation, $(\mathbf{I} - \mathbf{T})\boldsymbol{\theta} = \mathbf{0}$ or $(\mathbf{I} - \mathbf{D}^{-1}\mathbf{A})\boldsymbol{\theta} = \mathbf{0}$, whose solution is trivially $\boldsymbol{\theta} = p_o \mathbf{1}$. Equivalently, from the stochastic realization point-of-view, the probability of threat on all vertices is the same because average over all random walks between any vertex to a boundary (observed) vertex is trivially the observed, constant probability of threat p_o .

The following maximum principle establishes the existence of a unique non-negative threat probability on a graph given threat probabilities at observed vertices:

Theorem 1 (Maximum Principle for Threat Propagation).

Let $G = (V, E)$ be a connected graph with positive probability of threat $\theta_{v_{b_1}}, \dots, \theta_{v_{b_C}}$ at observed vertices v_{b_1}, \dots, v_{b_C} and the a priori probability ψ_v that threat propagates through vertex v . Then there exists a unique probability of threat θ_v at all vertices such that $\theta_v \geq 0$ and the maximum threat occurs at the observed vertices.

Proof: That θ_v exists follows from the connectivity of G , and that it takes its maximum on the boundary follows immediately from Eq. (14) because the threat at all vertices is necessarily bounded above by their neighbors. Now prove that θ_v is nonnegative by establishing a contradiction. Let θ_m be the minimum of all $\theta_v < 0$. Because $\psi_m \leq 1$, Eq. (14) implies that $\theta_m \geq \text{Avg}[N(m)]$, the weighted average value of the neighbors of m . Therefore, there exists a neighbor $n \in N(m)$ such that $\theta_n \leq \theta_m$. But θ_m is by assumption the minimum value. Therefore, $\theta_n = \theta_m$ for all $n \in N(m)$. Because G is connected, $\theta_v \equiv \theta_m$ is constant for all unobserved vertices on G . Now consider the minimum threat θ_i for which $i \in N(b)$

is a neighbor of an observed vertex b . By Eq. (14),

$$\theta_i = \psi_i d_i^{-1} \left(\sum_{j \in N(i) \setminus b} \theta_j + \theta_b \right), \quad (16)$$

$$\geq \psi_i d_i^{-1} ((d_i - 1)\theta_i + \theta_b). \quad (17)$$

Therefore,

$$\theta_i \geq \frac{\psi_i \theta_b}{(1 - \psi_i)d_i + \psi_i} \geq 0, \quad (18)$$

a contradiction. Therefore, the minimum value of θ_v is non-negative. ■

This theorem is intuitively appealing because it shows how nonuniform a priori probabilities ψ_v yield a nonconstant and nonnegative threat on the graph; however, the theorem conceals the crucial additional ‘‘absorbing’’ state that allows threat to dissipate away from the constant solution. This slight defect will be corrected shortly when the equivalent stochastic realization Markov chain model is introduced. Models about the likelihood of threat at specific vertices across the graph are provided by the a priori probabilities ψ_v , which as discussed above prevent the uninformative (yet valid) solution of constant threat across the graph given an observation of threat at a specific vertex.

A simple model for the a priori probabilities is degree-weighted threat propagation (DWTP),

$$\psi_v = \frac{1}{d_v} \quad (\text{DWTP}), \quad (19)$$

in which threat is less likely to propagate through high-degree vertices. Another simple model sets the mean propagation length proportional to the graph's average path length $l(G)$ yields length-weighted threat propagation (LWTP)

$$\psi_v \equiv 2^{-1/l(G)} \quad (\text{LWTP}). \quad (20)$$

For almost-surely connected Erdős–Rényi graphs with $p = n^{-1} \log n$, $l(G) = (\log n - \gamma)/\log \log n + 1/2$ and $\gamma = 0.5772\dots$ is Euler's constant [25]. A model akin to breadth-first search (BFS) sets the a priori probabilities to be inversely proportional to the Dijkstra distance from observed vertices, i.e.

$$\psi_v \propto 1/\text{dist}(v, \{v_{b_1}, \dots, v_{b_C}\}) \quad (\text{BFS}). \quad (21)$$

Defining the generalized Laplacian operator

$$\mathbf{L}^\psi \stackrel{\text{def}}{=} \mathbf{I} - \boldsymbol{\Psi} \mathbf{D}^{-1} \mathbf{A}, \quad (22)$$

the threat propagation equation Eq. (15) written as

$$\mathbf{L}^\psi \boldsymbol{\theta} = \mathbf{0}, \quad (23)$$

connects the generalized asymmetric Laplacian matrix of with threat propagation, the solution of which itself may be viewed as a boundary value problem with the harmonic operator \mathbf{L}^ψ . Given observations at vertices v_{b_1}, \dots, v_{b_C} , the *harmonic threat propagation equation* is

$$\left(\mathbf{L}_{ii}^\psi \mathbf{L}_{ib}^\psi \right) \begin{pmatrix} \theta_i \\ \theta_b \end{pmatrix} = \mathbf{0} \quad (24)$$

where the generalized Laplacian $\mathbf{L}^\psi = \begin{pmatrix} \mathbf{L}_{ii}^\psi & \mathbf{L}_{ib}^\psi \\ \mathbf{L}_{bi}^\psi & \mathbf{L}_{bb}^\psi \end{pmatrix}$ and the threat vector $\boldsymbol{\theta} = \begin{pmatrix} \theta_i \\ \theta_b \end{pmatrix}$ have been permuted so that observed

vertices are in the ‘b’ blocks (the “boundary”), unobserved vertices are in ‘i’ blocks (the “interior”), and the observation vector θ_b is given. The *harmonic threat* is the solution to Eq. (24),

$$\theta_i = -(\mathbf{L}_{ii}^\psi)^{-1}(\mathbf{L}_{ib}^\psi \theta_b). \quad (25)$$

Eq. (24) is directly analogous to Laplace’s equation $\Delta\varphi = 0$ given a fixed boundary condition. As discussed in the next subsection and Section II-B, the connection between threat propagation and harmonic graph analysis also provides a link to spectral-based methods for network detection. In practice, the highly sparse linear system of Eq. (25) may be solved by simple repeated iteration of Eq. (13), or using the biconjugate gradient method, which provides a practical computational approach that scales well to graphs with thousands of vertices and thousands of time samples in the case of space-time threat propagation, resulting in graphs of order ten million or more. In practice, significantly smaller subgraphs are encountered in applications such as threat network discovery [56], for which linear solvers with sparse systems are extremely fast.

2) *Stochastic Realization Approach*: The stochastic realization interpretation of the Bayesian threat propagation equations (13) is that the probability of threat for one random walk from v to the observed vertex v_{b_c} is

$$\theta_v \mid \text{walk}_{v \rightarrow v_{b_c}} = \theta_{v_{b_c}}, \quad (26)$$

and the probability of threat θ_v at v equals the threat probability averaged over all random walks emanating from v . This is equivalent to an absorbing Markov chain with absorbing states [49] at which random walks terminate. The absorbing vertices for the threat diffusion model are the C observed vertices, and an augmented state reachable by all unobserved vertices representing a transition from threat to non-threat with probability $1 - \psi_v$. The $(N+1)$ -by- $(N+1)$ transition matrix for the Markov chain corresponding to threat propagation equals

$$\mathbf{T} = \begin{array}{c} N-C \\ C \\ 1 \end{array} \begin{array}{ccc} N-C & C & 1 \\ \left(\begin{array}{ccc} \mathbf{G} & \mathbf{H} & \mathbf{1} - \psi_{N-C} \\ \mathbf{0} & \mathbf{I} & \mathbf{0} \\ \mathbf{0} & \mathbf{0} & 1 \end{array} \right) \\ \end{array} \quad (27)$$

in which \mathbf{G} and \mathbf{H} are defined by the block partition

$$\Psi \mathbf{D}^{-1} \mathbf{A} = \begin{array}{c} N-C \\ C \end{array} \begin{array}{cc} N-C & C \\ \left(\begin{array}{cc} \mathbf{G} & \mathbf{H} \\ * & * \end{array} \right) \\ \end{array} \quad (28)$$

with ‘*’ denoting unused blocks, and $\psi_{N-C} = (\psi_1, \psi_2, \dots, \psi_{N-C})^T$ is the vector of a priori threat diffusion probabilities from 1 to $N-C$. The observed vertices v_{b_1}, \dots, v_{b_C} are assigned to indices $N-C+1, \dots, N$, and the augmented “non-threat” state is assigned to index $N+1$.

According to this stochastic realization model, the threat at a vertex for any single random walk that terminates at an absorbing vertex is given by the threat level at the terminal vertex, with the augmented “non-threat” vertex assigned a threat level of zero; the threat is determined by this result averaged over all random walks. Ignoring the a priori probabilities, this is also precisely the stochastic realization model

for equilibrium thermodynamics and, in general, solutions to Laplace’s equation [47], [51].

As in Eq. (4), the uniform vector $(N+1)^{-1} \mathbf{1}_{N+1}$ is the left eigenvector of \mathbf{T} because \mathbf{T} is a right stochastic matrix, i.e. $\mathbf{T} \cdot \mathbf{1} = \mathbf{1}$. For an irreducible transition matrix of a strongly connected graph, the Perron–Frobenius theorem [26], [28] guarantees that this eigenvalue is simple and that the constant vector is the unique invariant eigenvector corresponding to $\lambda = 1$, a trivial solution that, as usual, poses a fundamental problem for network detection. However, neither version of the Perron–Frobenius theorem applies to the transition matrix \mathbf{T} of an absorbing Markov chain because \mathbf{T} is not strictly positive, as required by Perron, nor is \mathbf{T} irreducible, as required by Frobenius—the absorbing states are not strongly connected to the graph.

To guarantee the existence of nonnegative threat propagating over the graph, we require a generalization of the Perron–Frobenius theorem for reducible nonnegative matrices of the form found in Eq. (27). The following theorem introduces a new version of Perron–Frobenius that establishes the existence of a nonnegative basis for the principal invariant subspace of a reducible nonnegative matrix.

Theorem 2 (Perron–Frobenius for a Reducible Nonnegative Matrix). *Let \mathbf{T} be a reducible, nonnegative, order n matrix of canonical form,*

$$\mathbf{T} = \begin{pmatrix} \mathbf{Q} & \mathbf{R} \\ \mathbf{0} & \mathbf{I}_r \end{pmatrix}, \quad (29)$$

such that the maximum modulus of the eigenvalues of \mathbf{Q} is less than unity, $|\lambda_{\max}(\mathbf{Q})| < 1$, and $\text{rank } \mathbf{R} = r$. Then the maximal eigenvalue of \mathbf{T} is unity with multiplicity r and nondefective. Furthermore, there exists a nonnegative matrix

$$\mathbf{E} = \begin{pmatrix} (\mathbf{I} - \mathbf{Q})^{-1} \mathbf{R} \\ \mathbf{I}_r \end{pmatrix} \quad (30)$$

of rank r such that

$$\mathbf{T} \mathbf{E} = \mathbf{E}, \quad (31)$$

i.e. the columns of \mathbf{E} span the principal invariant subspace of \mathbf{T} .

The proof follows immediately by construction and a straightforward computation involving the partition $\mathbf{E} = \begin{pmatrix} \mathbf{E}_1 \\ \mathbf{E}_2 \end{pmatrix}$ with the choice $\mathbf{E}_2 = \mathbf{I}_r$, resulting in the nonnegative solution to Eq. (31), $\mathbf{E}_1 = (\mathbf{I} - \mathbf{Q})^{-1} \mathbf{R} = (\mathbf{I} + \mathbf{Q} + \mathbf{Q}^2 + \dots) \mathbf{R}$.

Theorem 2 has immediate application to threat propagation, for by definition the probability of threat on the graph is determined by the vector $\theta^a = \begin{pmatrix} \theta_i \\ \theta_b^a \end{pmatrix}$ such that $\mathbf{T} \theta^a = \theta^a$ and $\theta_b^a = \begin{pmatrix} \theta_b \\ 0 \end{pmatrix}$ is determined by the probabilities of threat $\theta_b = (\theta_{N-C+1}, \dots, \theta_N)^T$ at observed vertices v_{b_1}, \dots, v_{b_C} [cf. Eq. (24)] augmented with zero threat $\theta_{N+1}^a = 0$ at the “non-threat” vertex. From Eqs. (27) and (29), $\mathbf{Q} = \mathbf{G}$, $\mathbf{R} = (\mathbf{H} \ \mathbf{1} - \psi_{N-C})$, and $\mathbf{R} \theta_b^a = \mathbf{H} \theta_b$. Therefore, the vector that satisfies the proscribed boundary value problem equals

$$\theta^a = \begin{pmatrix} (\mathbf{I} - \mathbf{G})^{-1} \mathbf{H} \theta_b \\ \theta_b^a \end{pmatrix}. \quad (32)$$

As is well-known [49], the hitting probabilities of a random walk from an unobserved vertex to an observed vertex are given by the matrix $\mathbf{U} = (\mathbf{I} - \mathbf{G})^{-1}\mathbf{H}$; therefore, an equivalent definition of threat probability θ_v from Eq. (32) is the probability that a random walk emanating from v terminates at an observed vertex, conditioned on the probability of threat over all observed vertices:

$$\theta_v = \sum_c P(\text{walk}_{v \rightarrow v_{b_c}})P(\Theta_{v_{b_c}}). \quad (33)$$

We have thus proved the following theorem establishing the equivalence between the probabilistic and stochastic realization approaches of threat propagation.

Theorem 3 (Harmonic threat propagation). *The vector $\theta = \begin{pmatrix} \theta_i \\ \theta_b \end{pmatrix} \in \mathbb{R}^N$ is a solution to the boundary value problem of Eq. (24) if and only if the augmented vector $\theta^a = \begin{pmatrix} \theta_i \\ \theta_b^a \end{pmatrix} \in \mathbb{R}^{N+1}$ is a stationary vector of the absorbing Markov chain transition matrix \mathbf{T} of Eq. (27) with given values θ_b^a . Furthermore, θ is nonnegative.*

This theorem will also provide a connection to the spectral method for network detection discussed in Section II-B.

B. Space-Time Threat Propagation

Many important network detection applications, especially networks based on vehicle tracks and computer communication networks, involve directed graphs in which the edges have departure and arrival times associated with their initial and terminal vertices. Space-Time threat propagation is used compute the time-varying threat across a graph given one or more observations at specific vertices and times [48], [57]. In such scenarios, the time-stamped graph $G = (V, E)$ may be viewed as a *space-time graph* $G_T = (V \times T, E_T)$ where T is the set of sample times and $E_T \subset [V \times T]^2$ is an edge set determined by the temporal correlations between vertices at specific times. This edge set is application-dependent, but must satisfy the two constraints, (1) if $(u(t_k), v(t_l)) \in E_T$ then $(u, v) \in E$, and (2) temporal subgraphs $((u, v), E_T(u, v))$ between any two vertices u and v are defined by a temporal model $E_T(u, v) \subset [T \sqcup T]^2$. If the stronger, converse of property (1) holds, i.e. if $(u, v) \in E$ then either $(u(t_k), v(t_l)) \in E_T$ or $(v(t_l), u(t_k)) \in E_T$ for all t_k, t_l , then if the graph G is irreducible, then so is the space-time graph G_T . An example space-time graph is illustrated in Fig. 2. The general models for spatial threat propagation provided in the preceding subsection will now be augmented to include dynamic models of threat propagation.

Given an observed threat at a particular vertex and time, we wish to compute the inferred threat across all vertices and all times. Given a vertex v , denote the threat at v and at time $t \in \mathbb{R}$ by the $\{0, 1\}$ -valued stochastic process $\Theta_v(t)$, with value zero indicating no threat, and value unity indicating a threat. As above, denote the *probability of threat* at v at t by

$$\theta_v(t) \stackrel{\text{def}}{=} P(\Theta_v(t) = 1) = P(\Theta_v(t)). \quad (34)$$

The threat state at v is modeled by a finite-state continuous time Markov jump process between from state 1 to state 0

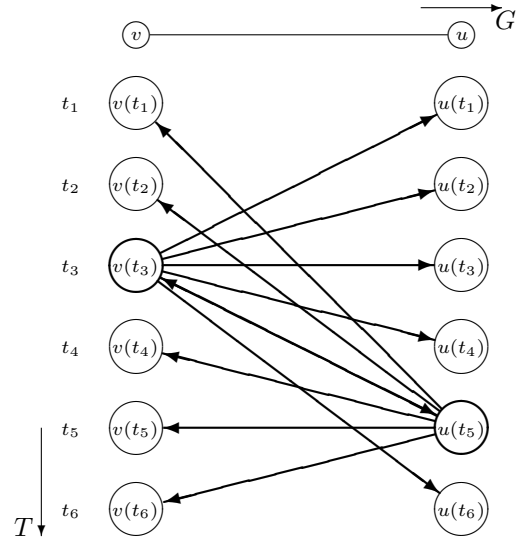


Fig. 2. A directed space-time graph G_T with vertices $V \times T$, $V = \{u, v\}$ sampled at index times $T = (t_1, \dots, t_6)$. For example, an interaction between $u(t_5)$ and $v(t_3)$ (represented by the doubled-sided arrow $v(t_3) \leftrightarrow u(t_5)$ above) also creates space-time edges via the space-time kernel [Eq. (36)] between $u(t_5)$ and other times at v , and $v(t_3)$ and other times at u .

with Poisson rate λ_v . With this simple model the threat stochastic process $\Theta_v(t)$ satisfies the Itô stochastic differential equation [60],

$$d\Theta_v = -\Theta_v dN_v; \quad \Theta_v(0) = \theta_1, \quad (35)$$

where $N_v(t)$ is a Poisson process with rate λ_v defined for positive time, and simple time-reversal provides the model for negative times. Given an observed threat $z = \Theta_v(0) = 1$ at v at $t = 0$ so that $\theta_v(0) = 1$, the probability of threat at v under the Poisson process model (including time-reversal) is

$$\theta_v(t) = P(\Theta_v(t) | z = \Theta_v(0) = 1) = e^{-\lambda_v |t|}, \quad (36)$$

This stochastic model provides a Bayesian framework for inferring, or propagating, threat at a vertex over time given threat at a specific time. The function

$$K_v(t) = e^{-\lambda_v |t|} \quad (37)$$

of Eq. (36) is called the *space-time threat kernel* and when combined with spatial propagation provides a temporal model E_T for a space-time graph. A Bayesian model for propagating threat from vertex to vertex will provide a full space-time threat diffusion model and allow for the application of the optimum maximum likelihood test that will be developed in Section III-D.

Propagation of threat from vertex to vertex is determined by interactions between vertices. Upon computation of the space-time adjacency matrix, the spatial analysis of Section III-A applies directly to space-time graphs whose vertices are space-time positions. The threat at vertex v at which a single interaction τ from vertex u arrives and/or departs at times t_τ^v and t_τ^u is determined by Eq. (36) and the (independent) event $\Psi_v(t)$ that threat propagates through v at time t : $P(\Theta_v(t)) = \theta_v(t) = \theta_u(t_\tau^u)K_v(t - t_\tau^v)\psi_v(t)$. There is a linear

transformation

$$\begin{aligned}\theta_v(t) &= \psi_{v(t)} K(t - t_\tau^v) \theta_u(t_\tau^u) \\ &= \int_{-\infty}^{\infty} \psi_{v(t)} K(t - t_\tau^v) \delta(\sigma - t_\tau^u) \theta_u(\sigma) d\sigma\end{aligned}\quad (38)$$

from the threat probability at u to v . Discretizing time, the temporal matrix \mathbf{K}_τ^{uv} for the discretized operator has the sparse form

$$\mathbf{K}_\tau^{uv} = \left(\mathbf{0} \dots \mathbf{0} K(t_k - t_\tau^v) \mathbf{0} \dots \mathbf{0} \right), \quad (39)$$

where $\mathbf{0}$ represents an all-zero column, t_k represents a vector of discretized time, and the discretized function $K(t_k - t_\tau^v)$ appears in the column corresponding to the discretized time at t_τ^u . Threat propagating from vertex v to u along the same interaction τ is given by the comparable expression $\theta_u(t) = \theta_v(t_\tau^v) K(t - t_\tau^u)$, whose discretized linear operator \mathbf{K}_τ^{vu} takes the form

$$\mathbf{K}_\tau^{vu} = \left(\mathbf{0} \dots \mathbf{0} K(t_k - t_\tau^u) \mathbf{0} \dots \mathbf{0} \right) \quad (40)$$

[cf. Eq. (39)] where the nonzero column corresponds to t_τ^v . The sparsity of \mathbf{K}_τ^{uv} and \mathbf{K}_τ^{vu} will be essential for practical space-time threat propagation algorithms. The collection of all interactions determines a weighted space-time adjacency matrix \mathbf{A} for the space-time graph G_T . This is a matrix of order $\#V \cdot \#T$ whose temporal blocks for interactions between vertices u and v equals,

$$\begin{pmatrix} \mathbf{A}_{uu} & \mathbf{A}_{uv} \\ \mathbf{A}_{vu} & \mathbf{A}_{vv} \end{pmatrix} = \begin{pmatrix} \mathbf{0} & \sum_l \mathbf{K}_{\tau_l}^{vu} \\ \sum_l \mathbf{K}_{\tau_l}^{uv} & \mathbf{0} \end{pmatrix}. \quad (41)$$

Note that with the space-time threat kernel of Eq. (37), if G is irreducible, then so is G_T .

As with spatial-only threat propagation of Eq. (13), the *space-time threat propagation equation* is

$$\boldsymbol{\theta} = \boldsymbol{\Psi} \mathbf{W}^{-1} \mathbf{A} \boldsymbol{\theta} \quad (42)$$

$$\text{or } \theta_v(t_k) = \frac{\psi_v(t_k)}{\sum_{u,l} k_{vu;kl}} \sum_{u,l} k_{vu;kl} \theta_u(t_l) \quad (43)$$

in which $\boldsymbol{\theta}$ is the (discretized) space-time vector of threat probabilities, $\mathbf{A} = (k_{vu;kl})$ is the (weighted) space-time adjacency matrix, and $\mathbf{W} = \text{Diag}(\mathbf{A} \cdot \mathbf{1})$ and $\boldsymbol{\Psi} = \text{diag}(\psi_1(t_1), \dots, \psi_N(t_{\#T}))$ are, respectively, the space-time diagonal matrices of the space-time vertex weights and a priori probabilities that threat propagates through each spatial vertex at a specific time. In contrast to the treatment of spatial-only threat propagation in Section III-A, the space-time graph is necessarily a directed graph, consistent with the asymmetric space-time adjacency matrix of Eq. (41).

By assumption, the graph G is irreducible, implying that the space-time graph G_T is also irreducible. Therefore, Theorem 1 implies a well-defined solution to the space-time threat propagation equation of Eq. (42) for a set observations at specific vertices and times, $v_{b_1}(t_{b_1}), \dots, v_{b_C}(t_{b_C})$. Yet the Perron–Frobenius theorem for the space-time Laplacian $\mathbf{L} = \mathbf{I} - \mathbf{W}^{-1} \mathbf{A}$ poses precisely the same detection challenge as with spatial-only propagation: if the a priori probabilities are constant and equal to unity, i.e. $\boldsymbol{\Psi} = \mathbf{I}$, and the observed

probability of threat is constant, then the space-time probability of threat is also constant for all spatial vertices and all times, yielding a hopeless detection method.

However, the advantage of time-stamped edges is that the times can be used to detected temporally coordinated network activity—we seek to detect vertices whose activity is correlated with that of threat observed at other vertices. According to this model of threat networks, the a priori probability that a threat propagates through vertex v at time t_k is determined by the Poisson process used to model the probability of threat as a function of time:

$$\psi_v(t_k) = \frac{1}{d_v} \sum_{u,l} k_{vu;kl}, \quad (44)$$

where d_v is the spatial degree of vertex v , i.e. the number of interactions associated with a spatial vertex. If all interactions arrive/depart at the same time at v , then the a priori probability of threat diffusion is unity at this time, but different times reduce this probability according to the stochastic process for threat. Thus space-time threat propagation for coordinated activity is determined by the threat propagation equation,

$$\boldsymbol{\theta} = \mathbf{D}^{-1} \mathbf{A} \boldsymbol{\theta} \quad (45)$$

in which $\mathbf{D} = \text{diag}(d_1 \mathbf{I}, \dots, d_N \mathbf{I})$ is the block-diagonal space-time matrix of (unweighted) spatial degrees and \mathbf{A} is the weighted space-time adjacency matrix as in Eq. (42). This algorithm may also be further generalized to account for spatial-only a priori probability models such as the distance from observed vertices by replacing $1/d_v$ in Eq. (45) with ψ'_v/d_v and an a priori model as in Eq. (19), yielding the threat propagation equation $\boldsymbol{\theta} = \boldsymbol{\Psi}' \mathbf{D}^{-1} \mathbf{A} \boldsymbol{\theta}$ with $\boldsymbol{\Psi}' = \text{diag}(\psi'_1 \mathbf{I}, \dots, \psi'_N \mathbf{I})$.

C. Hybrid Threat Propagation

The temporal kernels introduced for time-stamped edges in Section III-B are appropriate for network detection applications that involve time-stamped edges; however, there are many applications in which such time-stamped information is either unavailable, irrelevant, or uncertain. Ignoring small routing delays, computer network communication protocols occur essentially instantaneously, and text documents may describe relationships between sites independent of a specific timeframe. Integrating spatio-temporal relationships from multiple information sources necessitates a hybrid approach combining, where appropriate, the spatial-only capabilities of Section III-A with the space-time methods of Section III-B.

In situations such as computer communication networks in which the timescale of the relationship is much smaller than the discretized timescale, then connections from one vertex to another arrive at the same discretized time, and the temporal blocks for connections between vertices u and v replaces Eq. (41) and equals,

$$\begin{pmatrix} \mathbf{A}_{uu} & \mathbf{A}_{uv} \\ \mathbf{A}_{vu} & \mathbf{A}_{vv} \end{pmatrix} = \begin{pmatrix} \mathbf{0} & \mathbf{I} \\ \mathbf{I} & \mathbf{0} \end{pmatrix}. \quad (46)$$

In situations such as time-independent references within text documents in which threat at any time at vertex u implies a

threat at all times at vertex v , and vice versa, the temporal blocks for connections between vertices u and v equals,

$$\begin{pmatrix} \mathbf{A}_{uu} & \mathbf{A}_{uv} \\ \mathbf{A}_{vu} & \mathbf{A}_{vv} \end{pmatrix} = \begin{pmatrix} \mathbf{0} & (\#T)^{-1} \mathbf{1}\mathbf{1}^\top \\ (\#T)^{-1} \mathbf{1}\mathbf{1}^\top & \mathbf{0} \end{pmatrix}, \quad (47)$$

i.e. a space-time clique between u and v . This equivalent the space-time model with Poisson rate $\lambda = 0$.

D. Neyman–Pearson Network Detection

Network detection of a subgraph within a graph $G = (V, E)$ of order N is treated as N independent binary hypothesis tests to decide which of the graph's N vertices do not belong (null hypothesis H_0) or belong (hypothesis H_1) to the network. Maximizing the probability of detection (PD) for a fixed probability of false alarm (PFA) yields the Neyman–Pearson test involving the log-likelihood ratio of the competing hypotheses. We will derive this test in the context of network detection, which both illustrates the assumptions that ensure detection optimality, as well as indicates practical methods for computing the log-likelihood ratio test and achieving an optimal network detection algorithm. It will be seen that a few basic assumptions yield an optimum test that is equivalent to the Bayesian threat propagation algorithm developed in the previous section. If any part of the graph is unknown or uncertain, then the Markov transition probabilities may be treated as random variables and either marginalized out of the likelihood ratio, yielding Neyman–Pearson optimality in the average sense, or the maximum likelihood estimate may be used in the suboptimum generalized likelihood ratio test (GLRT) [63]. We will not cover extensions to unknown parameters in this paper. The optimum test involves the graph Laplacian, which allows comparison of Neyman–Pearson testing to several other network detection methods whose algorithms are also related to the properties of the Laplacian.

An optimum hypothesis test is now derived for the presence of a network given a set of observations \mathbf{z} according to the observation model of Definition 4. Optimality is defined in the Neyman–Pearson sense in which the probability of detection is maximized at a constant false alarm rate (CFAR) [63]. For the general problem of network detection of a subgraph within graph G of order N , the decision of which of the 2^N hypothesis $\Theta = (\Theta_{v_1}, \dots, \Theta_{v_N})^\top$ to choose involves a 2^N -ary multiple hypothesis test over the measurement space of the observation vector \mathbf{z} , and an optimal test involves partitioning the measurement space into 2^N regions yielding a maximum PD. This NP-hard general combinatoric problem is clearly computationally and analytically intractable. However, Eq. (11) following Definition 6 guarantees that the threats at each vertex are independent random variables, allowing the general 2^N -ary multiple hypothesis test to be greatly simplified by treating it as N independent binary hypothesis tests at each vertex.

At each vertex $v \in G$ and unknown threat $\Theta: V \rightarrow \{0, 1\}$ across the graph, consider the binary hypothesis test for the unknown value Θ_v ,

$$\begin{aligned} H_0(v): \quad & \Theta_v = 0 && \text{(vertex belongs to background)} \\ H_1(v): \quad & \Theta_v = 1 && \text{(vertex belongs to foreground).} \end{aligned} \quad (48)$$

Given the observation vector $\mathbf{z}: \{v_{b_1}, \dots, v_{b_C}\} \subset V \rightarrow M \subset \mathbb{R}^C$ with observation models $f(z(v_{b_j}) \mid \Theta_{v_{b_j}})$, $j = 1, \dots, C$, the PD and PFA are given by the integrals $\text{PD} = \int_R f(\mathbf{z} \mid \Theta_v = 1) d\mathbf{z}$ and $\text{PFA} = \int_R f(\mathbf{z} \mid \Theta_v = 0) d\mathbf{z}$, where $R \subset M$ is the detection region in which observations are declared to yield the decision $\Theta_v = 1$, otherwise Θ_v is declared to equal 0. The optimum Neyman–Pearson test uses the detection region R that maximizes PD at a fixed CFAR value PFA_0 , yielding the likelihood ratio (LR) test [63],

$$\frac{f(\mathbf{z} \mid \Theta_v = 1)}{f(\mathbf{z} \mid \Theta_v = 0)} \underset{H_0(v)}{\overset{H_1(v)}{\geq}} \lambda \quad (49)$$

for some $\lambda > 0$. Likelihood ratio tests are also used for graph classification [36].

Finally, a simple application of Bayes' theorem to the harmonic threat $\theta_v = f(\Theta_v \mid \mathbf{z})$ provides the optimum Neyman–Pearson detector [Eq. (49)] because

$$\begin{aligned} \frac{f(\mathbf{z} \mid \Theta_v = 1)}{f(\mathbf{z} \mid \Theta_v = 0)} &= \frac{f(\Theta_v = 1 \mid \mathbf{z})}{f(\Theta_v = 0 \mid \mathbf{z})} \cdot \frac{f(\Theta_v = 0)}{f(\Theta_v = 1)} \\ &= \frac{\theta_v}{1 - \theta_v} \cdot \frac{f(\Theta_v = 1)}{f(\Theta_v = 0)} \underset{H_0(v)}{\overset{H_1(v)}{\geq}} \lambda, \end{aligned} \quad (50)$$

results in a threshold of the harmonic space-time threat propagation vector of Eq. (7),

$$\theta_v \underset{H_0(v)}{\overset{H_1(v)}{\geq}} \text{threshold}, \quad (51)$$

with the prior ratio $f(\Theta_v = 1)/f(\Theta_v = 0)$ and the monotonic function $\theta_v \mapsto \theta_v/(1 - \theta_v)$ being absorbed into the detection threshold. By construction, the event $\Theta_v = 1$ is equivalent to a random walk between v and one of the observed vertices v_{b_1}, \dots, v_{b_C} , along with one of the events $\Theta_{v_{b_1}} = 1, \dots, \Theta_{v_{b_C}} = 1$, as represented in Eq. (33). Note that θ_v and equivalently the likelihood ratio are continuous functions of the probabilities $P(\text{walk}_{v \rightarrow v_{b_c}})$ and $P(\Theta_{v_{b_c}})$; therefore, equality of the likelihood ratio to any given threshold exists only on a set of measure zero. If the prior ratio is constant for all vertices, then the threshold is also constant, and the likelihood ratio test [Eq. (51)] for optimum network detection becomes

$$\theta \underset{H_0}{\overset{H_1}{\geq}} \text{threshold}. \quad (52)$$

This establishes the detection optimality of harmonic space-time threat propagation.

Because the probability of detecting threat is maximized at each vertex, the probability of detection for the entire subgraph is also maximized, yielding an optimum Neyman–Pearson test under the simplification of treating the 2^N -ary multiple hypothesis testing problem as a sequence of N binary hypothesis tests. Summarizing, the probability of network detection given an observation \mathbf{z} is maximized by computing $f(\Theta_v \mid \mathbf{z})$ using a Bayesian threat propagation method and applying a simple likelihood ratio test, yielding the following theorem that equates threat propagation with the optimum Neyman–Pearson test.

Theorem 4 (Neyman–Pearson Optimality of Threat Propagation). *The solution to Bayesian threat propagation expressed in Eqs. (24) or (32) yields an optimum likelihood ratio test in the Neyman–Pearson sense.*

IV. MODELING AND PERFORMANCE

Evaluation of network detection algorithms may be approached from the perspectives of theoretical analysis or empirical experimentation. Theoretical performance bounds have only been accomplished for simple network models, i.e. cliques [23], [33], [42] or dense subgraphs [5] embedded within Erdős–Rényi backgrounds, and there are no theoretical results at all for more complex network models that characterize real-world networks [58]. If representative network data with truth is available, one may evaluate algorithm performance with specific data sets [71]. However, real-world data sets of covert networks with truth is unknown to the authors. Therefore, network detection performance evaluation must be conducted on simulated networks using generative models. We begin with a simple stochastic blockmodel [65], explore this model’s limitations, then introduce a new network model designed to address these defects while at the same time encompassing the characteristics of real-world networks [1], [2], [12], [45], [70]. Varying model parameters also yields insight on the dependence of algorithm performance on different network characteristics.

For each evaluation, we compare performance between the space-time threat propagation [STTP; Section III-B], breadth-first search spatial-only threat propagation [BFS; Eq. (21)], and modularity-based spectral detection algorithm [SPEC] [40]. The performance metric is the standard receiver operating characteristic (ROC), which in the case of network detection is the probability of detection (i.e. the percentage of true foreground vertices detected) versus the probability of false alarms (i.e. the percentage of background vertices detected) as the detection threshold is varied.

A. Detection Performance On Stochastic Blockmodels

1) *Stochastic Blockmodel Description:* The stochastic blockmodel captures the sparsity of real-world networks and basic community structure [27] using a simple network framework [65]. For a graph of order N divided into K communities, the model is parameterized by a N -by- K $\{0, 1\}$ membership matrix $\mathbf{\Pi}$ and a K -by- K probability matrix \mathbf{S} that defines the probability of an edge between two vertices based upon their community membership. Therefore, the probability of an edge is determined by the off-diagonal terms of the matrix $\mathbf{\Pi}\mathbf{S}\mathbf{\Pi}^T$. By the classical result of Erdős–Rényi [20], each community is almost surely connected if $\mathbf{S}_{kk} > \log N_k/N_k$ in which N_k is the number of vertices in community k . We introduce the activity parameter $r_k \geq 1$ and set $\mathbf{S}_{kk} = r_k \log N_k/N_k$ to adjust a community’s density relative to its Erdős–Rényi connectivity threshold.

2) *Experimental Setup and Results:* The objective of this experiment is to quantify detection performance of a foreground network with varying activity given observations from a small fraction of its members. Fig. 3 illustrates the ROC

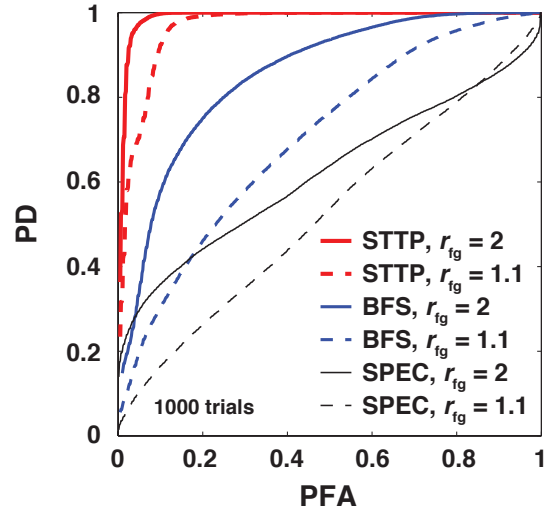


Fig. 3. Detection ROC curves of the three different algorithms at two levels of foreground activity, $1.1 \cdot \log N_{fg}/N_{fg}$ and $2 \cdot \log N_{fg}/N_{fg}$. Data is simulated using the stochastic blockmodel with 1000 Monte Carlo trials each with an independent draw of the random network and single threat observation.

detection performance with a graph of order $N = 256$ and $K = 3$ with two background communities of order 128, and a foreground community of order 30 randomly embedded in the background. The probability matrix is,

$$\mathbf{S} = \begin{pmatrix} 0.08 & 0.02 & 0.02 \\ 0.02 & 0.08 & 0.02 \\ 0.02 & 0.02 & r_{fg} \cdot 0.1 \end{pmatrix},$$

parameterized by the activity r_{fg} relative to the Erdős–Rényi foreground connectivity threshold $\log 30/30 \approx 0.1$. A simple temporal model is used with all foreground interactions at the same time (i.e. perfect coordination), and background interactions uniformly distributed in time (i.e. uncoordinated).

Results are shown for both sparsely connected ($r_{fg} = 1.1$) and moderately connected ($r_{fg} = 2$) foreground networks. The simulations show that excellent ROC performance is achievable if temporal information is exploited (STTP) with highly coordinated foreground networks with sparse to moderate connectivity. Because of the use of temporal information, STTP outperforms BFS. Spectral methods, which are designed to detect highly connected networks perform poorly on sparse foreground networks, and improve as foreground network connectivity increases, especially in the low PFA region in which SPEC performs better than BFS threat propagation. This result is consistent with expectations and recent theoretical results for spectral methods applied to clique detection [5], [42]. Continuous likelihood ratio tests possess ROC curves that are necessarily convex upwards [63]; therefore, the ROCs for threat propagation algorithms applied to data generated from random walk propagation are necessarily convex. The results of Fig. 3 show both threat propagation and spectral methods applied to data generated from a stochastic blockmodel. Because the spectral detection algorithm is not associated with a likelihood ratio test, convexity of its ROC curves is not guaranteed—indeed, the spectral ROC curve with $r_{fg} = 2$ is seen to be concave in the high PD region. All threat

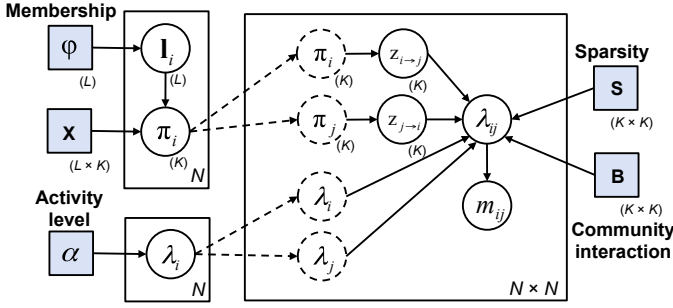


Fig. 4. Hybrid mixed-membership blockmodel for the network simulation with N vertices, K communities, and L lifestyles. Shaded squares are model parameters for tuning and circles are variables drawn during simulation.

propagation ROC curves are observed to be convex, except for a small part of STTP with $r_{fg} = 1.1$ near $PD = 0.7$. This slight concavity (about 2%) may be caused by model mismatch between the stochastic blockmodel and the random walk model, or statistical fluctuation of the Monte Carlo analysis (about 1.4% binomial distribution variance at $PD = 0.7$).

Of course, real-world networks are not perfectly coordinated, ideal Erdős–Rényi graphs. We will develop a novel, more realistic model in the next section to explore how more realistic networks with varying levels of foreground coordination affect the performance of space-time threat propagation.

B. Detection Performance on the Hybrid Mixed-Membership Blockmodel

1) Hybrid Mixed-Membership Blockmodel Description:

Real-world networks display basic topological characteristics that include a power-law degree distribution (i.e. the “small world” property) [12], mixed-membership-based community structure (i.e. individuals belong to multiple communities) [2], [65], and sparsity [44]. No one simple network model captures all these traits. For example, the stochastic blockmodel above provides sparsity and a rough community structure, but does not capture interactions through time, the power-law degree distribution, nor the reality that each individual may belong to multiple communities. The power-law models such as R-MAT [12] do not capture membership-based community structure, and mixed-membership stochastic blockmodels [2] does not capture power-law degree distribution nor temporal coordination. To capture all these characteristics of the real-world networks model, we propose a new parameterized generative model called the “hybrid mixed-membership blockmodel” (HMMB) that combines the features of these fundamental network models. The proposed model is depicted as the plate diagram in Fig. 4.

The hybrid mixed-membership blockmodel is an aggregate of the following simpler models and their features: Erdős–Rényi for sparsity [20], Chung–Lu for power-law degree distribution [1], and mixed-membership stochastic blockmodel for community structure [2]. We model the number of interactions between any two individuals (i.e. edge weights) as Poisson random variables. Each interaction receives a timestamp through a coordination model. As above, let N be the order of the graph, and let K be the number of communities. Each individual (i.e.

vertex) divides its membership among the K communities (i.e. mixed membership), and the fraction in which an individual participates among the different communities is determined by L distinct lifestyles. The rate λ_{ij} of interactions between vertices i and j is given by the product

$$\lambda_{ij} = I_{ij}^S \cdot \frac{\lambda_i \lambda_j}{\sum_k \lambda_k} \cdot \mathbf{z}_{i \rightarrow j}^T \mathbf{B} \mathbf{z}_{j \rightarrow i}, \quad (53)$$

where the first term I_{ij}^S is the (binary) indicator function drawn from the stochastic blockmodel described in Section IV-A, the second term $\lambda_i \lambda_j / (\sum_k \lambda_k)$ is the Chung–Lu model with per-vertex expected degrees λ_i , and the third term $\mathbf{z}_{i \rightarrow j}^T \mathbf{B} \mathbf{z}_{j \rightarrow i}$ is the mixed-membership stochastic blockmodel with K -by- K block matrix \mathbf{B} that determines the intercommunity interaction strength, and $\mathbf{z}_{i \rightarrow j}$ is a $\{0, 1\}$ -valued K -vector that indicates which community membership that vertex i assumes when interacting with vertex j .

The mixed-membership K -vector π_i specifies the fraction that individual vertex i divides its membership among the K communities so that $\mathbf{1}^T \pi_i \equiv 1$. Each vertex is assigned, via the $\{0, 1\}$ -valued L -vector \mathbf{l}_i , to one of L “lifestyles” each with an expected membership distribution given by the L -by- K matrix \mathbf{X} . The membership distribution π_i is determined by a Dirichlet random draw using the K -vector $\mathbf{l}^T \mathbf{X}$. The lifestyle vector \mathbf{l}_i is determined from a multinomial random draw using the L -vector ϕ as the probability of belonging to each lifestyle. Similarly, for each interaction, the community indicator vector $\mathbf{z}_{i \rightarrow j}$ is determined from a multinomial random draw using the K -vector π_i as the probability of belonging to each community. The expected vertex degrees λ_i are determined from a power-law random draw using the exponent α . The parameter matrices \mathbf{S} and \mathbf{B} are fixed.

Finally, intracommunity coordination is achieved by the nonnegative K -vector γ , a Poisson parameter of the average number of coordinated events at each vertex within a specific community. Smaller values of γ_k correspond to higher levels of coordination in community k because there are fewer event times from which to choose. A community-dependent Poisson random draw determines the integer number of event times within each community, which are then drawn uniformly over the time extent of interest. An edge between vertices i and j is assigned two random event timestamps based on the community indicator vectors $\mathbf{z}_{i \rightarrow j}$ and $\mathbf{z}_{j \rightarrow i}$.

2) *Experimental Setup and Results:* The objective of this experiment is to quantify detection performance with varying coordination of a realistic foreground network operating within a realistic background. We use eleven “lifestyles” spanning ten communities, with two lifestyles designated as foreground and all others as background.

The foreground network’s coordination varies from $\gamma_{fg} = 1$ (i.e. highly coordinated activity at a single time, consistent with the tactic used by covert networks to mitigate their exposure to discovery) to $\gamma_{fg} = 24$ (i.e. less coordination). Each member of the covert foreground network is also a member of several background communities. The foreground and background order are the same as in the experiment of Section IV-A2, and sparsity levels all $\log N_i / N_i$. The foreground network is only a small fraction of the entire population.

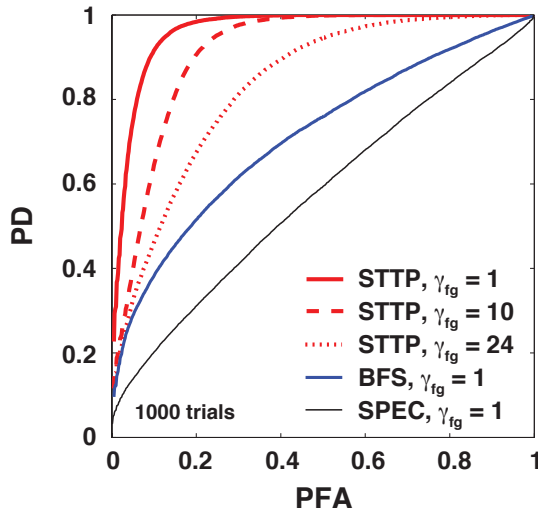


Fig. 5. Detection ROC curves of the three different algorithms at three levels ($\gamma_{fg} = 1, 10, 24$) of foreground coordination. Spectral detection and BFS threat propagation do not use temporal information so their performance is unaffected by the coordination level.

Foreground actors are characterized by two distinct lifestyles representing their memberships in the covert community as well as different background communities. The background communities are intended to represent various business, home, industry, religious, sports, or other social interactions.

Fig. 5 illustrates the ROC performance with these parameters, varying the level of foreground coordination. Through Eq. (44), space-time threat propagation is designed to perform well with highly coordinated networks, consistent with the results observed in Fig. 5 in which STTP performs best at the higher coordination levels and outperforms the breadth-first search and modularity-based spectral detection methods. The spectral detection algorithm is expected to perform poorly in this scenario because, as discussed in Section II-B, it relies upon a relatively dense foreground network, which does not exist in this simulated dataset with realistic properties of covert networks.

V. CONCLUSIONS

A Bayesian framework for network detection can be used to unify the different approaches of network detection algorithms based on random walks/diffusion and algorithms based on spectral properties. Indeed, using the concise assumptions for random walks and threat propagation laid out in Definition 6, all the theoretical results follow immediately, including the proof of equivalence, an exact, closed-form, efficient solution, and Neyman–Pearson optimality. Not only is this theoretically appealing, but it provides direct practical benefits through a new network detection algorithm called space-time threat propagation, that is shown to achieve superior performance with simulated covert networks. Bayesian space-time threat propagation is interpreted both as a random walk on a graph and, equivalently, as the solution to a harmonic boundary value problem. Bayes’ rule determines the unknown probability of threat on the uncued nodes—the “interior”—based on threat

observations at cue nodes—the “boundary.” Hybrid threat propagation algorithms appropriate for heterogeneous spatio-temporal relationships can be obtained from this general threat diffusion model. This new method is compared to well-known spectral methods by examining competing notions of network detection optimality. To model realistic covert networks realistically embedded within realistic backgrounds, a new hybrid mixed-membership blockmodel based on mixed membership of random graphs is introduced and used to assess algorithm detection performance on graphs with varying activity and coordination. In the important situations of low foreground activity with varying levels of coordination, the examples show the superior detection performance of Bayesian space-time threat propagation compared to other spatial-only and uncued spectral methods.

ACKNOWLEDGMENTS

The authors gratefully acknowledge the consistently incisive and constructive comments from our reviewers, which greatly improved this paper. We also thank Professor Patrick Wolfe for originally suggesting the deep connection with random walks on graphs.

REFERENCES

- [1] W. AIELLO, F. CHUNG, and L. LU. “A random graph model for power law graphs,” *Experimental Mathematics* **10** (1): 53–66 (2001).
- [2] E. M. AIROLDI, D. M. BLEI, S. E. FIENBERG, and E. P. XING. “Mixed-membership stochastic blockmodels,” *JMLR* **9**: 1981–2014 (2008).
- [3] M. ALANYALI, S. VENKATESH, O. SAVAS, and S. AERON. “Distributed Bayesian hypothesis testing in sensor networks,” in *Proc. 2005 American Control Conf.* Boston MA, pp. 5369–5374 (2004).
- [4] R. ANDERSEN, F. R. K. CHUNG, and K. LANG. “Local graph partitioning using PageRank vectors,” in *Proc. 47th IEEE Symp. Foundations of Computer Science (FOCS)*. pp. 475–486 (2006).
- [5] E. ARIAS-CASTRO and N. VERZELEN. “Community detection in random networks,” *arXiv:1302.7099 [math.ST]*. Mar. 18 2013 [Online]. Available: <http://arxiv.org/abs/1302.7099>.
- [6] S. ARORA, S. RAO, and U. VAZIRANI. “Geometry, flows, and graph-partitioning algorithms,” *Comm ACM* **51** (10): 96–105 (2008).
- [7] K. AVRACHENKOV, N. LITVAK, M. SOKOL, and D. TOWSLEY. “Quick detection of nodes with large degrees,” *Internet Mathematics* doi:10.1080/15427951.2013.798601, 12 Nov. 2013. Feb. 27 2014 [Online]. Available: <http://www.tandfonline.com/doi/abs/10.1080/15427951.2013.798601>.
- [8] M. BELKIN and P. NIYOGI. “Laplacian eigenmaps for dimensionality reduction and data representation,” *Neural Computation* **15**: 1373–1396 (2003).
- [9] K. CARLEY. “Estimating vulnerabilities in large covert networks,” in *Proc. 16th Intl. Symp. Command and Control Research and Tech. (ICCRTS)*. (San Diego, CA) (2004).
- [10] K. M. CARTER, R. RAICH, and A. O. HERO III. “On local intrinsic dimension estimation and its applications,” *IEEE Trans. Signal Processing* **58** (2): 650–663 (2010).
- [11] D. CHAKRABARTI, Y. WANG, C. WANG, J. LESKOVEC, and C. FALOUTSOS. “Epidemic thresholds in real networks,” *ACM T. Inform. Syst. Se.*, **10** (4): 13.1–13.26 (2008).
- [12] D. CHAKRABARTI, Y. ZHAN, and C. FALOUTSOS. “R-MAT: A recursive model for graph mining,” in *Proc. 2004 SIAM Intl. Conf. Data Mining*. pp. 442–446 (2004).
- [13] J.-F. CHAMBERLAND and V. V. VEERAVALLI. “Decentralized detection in sensor networks,” *IEEE Trans. Signal Processing* **51** (2): 407–416 (2003).
- [14] F. R. K. CHUNG. *Spectral Graph Theory*. Regional Conference Series in Mathematics **92**. Providence, RI: American Mathematical Society (1994).

- [15] F. R. K. CHUNG and W. ZHAO. "PageRank and random walks on graphs," in *Fete of Combinatorics and Computer Science*, Bolyai Society Mathematical Studies **20**: 43–62, Vienna: Springer (2010).
- [16] J. A. COSTA and A. O. HERO III. "Geodesic entropic graphs for dimension and entropy estimation in manifold learning," *IEEE Trans. Signal Processing* **52**(8): 2210–2221 (2004).
- [17] R. DIESTEL. *Graph Theory*. New York: Springer-Verlag, Inc. (2000).
- [18] W. E. DONATH and A. J. HOFFMAN. "Lower bounds for the partitioning of graphs," *IBM J. Res. Development* **17**: 420–425 (1973).
- [19] E. B. DYNKIN and A. A. YUSHKEVICH. *Markov Processes: Theorems and Problems*. New York: Plenum Press (1969).
- [20] P. ERDŐS and A. RÉNYI. "On the evolution of random graphs," *Pubs. Mathematical Institute of the Hungarian Academy of Sciences* **5**: 17–61 (1960).
- [21] J. P. FERRY, D. LO, S. T. AHEARN, and A. M. PHILLIPS. "Network detection theory," in *Mathematical Methods in Counterterrorism*, eds. N. MEMON *et al.*, pp. 161–181, Vienna: Springer (2009).
- [22] M. FIEDLER. "A property of eigenvectors of non-negative symmetric matrices and its application to graph theory," *Czech. Math. J.* **25**: 619–633 (1975).
- [23] S. FORTUNATO and M. BARTHÉLEMY. "Resolution limit in community detection," *PNAS* **104**(1): 36–41 (2007).
- [24] S. FORTUNATO. "Community detection in graphs," *Physics Reports* **486**: 75–174 (2010).
- [25] A. FRONCZAK, P. FRONCZAK, and J. A. HOŁYST. "Average path length in random networks," *Phys. Rev. E* **70**: 056110 (2004).
- [26] F. R. GANTMACHER. *Matrix Theory*. Vol. 2. New York: Chelsea (1959).
- [27] M. GIRVAN and M. E. J. NEWMAN. "Community structure in social and biological networks," *PNAS* **99**(12): 7821–7826 (2002).
- [28] C. GODSIL and G. ROYLE. *Algebraic Graph Theory*. New York: Springer-Verlag, Inc. (2001).
- [29] M. O. JACKSON. *Social and Economic Networks*, Princeton U. Press (2008).
- [30] A. SANDRYHAILA and J. F. MOURA. "Discrete signal processing on graphs: Frequency analysis," *IEEE Trans. Signal Processing* **62**(12): 3042–3054 (2014).
- [31] D. KOLLER and N. FRIEDMAN. *Probabilistic Graphical Models*. Cambridge, MA: MIT Press (2009).
- [32] V. E. KREBS. "Uncloaking terrorist networks," *First Monday* **7**(4) (2002), Feb. 27 2014 [Online]. Available: (<http://firstmonday.org/ojs/index.php/fm/article/view/941>).
- [33] J. M. KUMPULA, J. SARAMÄKI, K. KASKI, and J. KERTÉSZ. "Limited resolution in complex network community detection with Potts model approach," *Eur. Phys. J. B* **56**: 41–45 (2007).
- [34] J. LESKOVEC and C. FALOUTSOS. "Sampling from large graphs," in *Proc. 12th ACM SIGKDD Intl. Conf. Knowledge Discovery and Data Mining* pp. 631–636 (2006).
- [35] J. LESKOVEC, K. J. LANG, and M. MAHONEY. "Empirical comparison of algorithms for network community detection," in *Proc. 19th Intl. Conf. World Wide Web (WWW'10)*, Raleigh, NC, pp. 631–640 (2010).
- [36] J. G. LIGO, G. K. ATIA, and V. V. VEERAVALLI. "A controlled sensing approach to graph classification," in *Proc. IEEE Intl. Conf. Acoustics, Speech and Signal Processing (ICASSP)*, Vancouver, BC (2013).
- [37] M. W. MAHONEY, L. ORECCHIA, and N. K. VISHNOI. "A local spectral method for graphs: With applications to improving graph partitions and exploring data graphs locally," *J. Machine Learning Research* **13**: 2339–2365 (2012).
- [38] B. A. MILLER, M. S. BEARD, and N. T. BLISS. "Eigenspace Analysis for Threat Detection in Social Networks," in *Proc. 14th Intl. Conf. Informat. Fusion (FUSION)*, Chicago, IL (2011).
- [39] B. A. MILLER, N. T. BLISS, and P. J. WOLFE. "Toward signal processing theory for graphs and other non-Euclidean data," in *Proc. IEEE Intl. Conf. Acoustics, Speech and Signal Processing*, pp. 5414–5417 (2010).
- [40] B. A. MILLER, N. T. BLISS, and P. J. WOLFE. "Subgraph detection using eigenvector L_1 norms," in *Proc. 2010 Neural Information Processing Systems (NIPS)*, Vancouver, Canada (2010).
- [41] B. MOHAR. "The Laplacian Spectrum of Graphs," in *Graph Theory, Combinatorics, and Applications*, **2**, eds. Y. ALAVI, G. CHARTRAND, O. R. OELLERMANN, and A. J. SCHWENK. New York: Wiley, pp. 871–898 (1991).
- [42] R. R. NADAKUDITI and M. E. J. NEWMAN. "Graph spectra and the detectability of community structure in networks," *Phys. Rev. Lett.* **108**, 188701 (2012).
- [43] J. NEVILLE, O. SIMSEK, D. JENSEN, J. KOMOROSKE, K. PALMER, and H. GOLDBERG. "Using relational knowledge discovery to prevent securities fraud," in *Proc. 11th ACM SIGKDD Intl. Conf. Knowledge Discovery and Data Mining* pp. 449–458 (2005).
- [44] M. E. J. NEWMAN. "Finding community structure in networks using the eigenvectors of matrices," *Phys. Rev. E*, **74**(3) (2006).
- [45] ———. "The structure and function of complex networks," *SIAM Rev.* **45**(2): 167–256 (2003).
- [46] J.-P. ONNELA and N. A. CHRISTAKIS. "Spreading paths in partially observed social networks," *Phys. Rev. E*, **85**(3): 036106 (2012).
- [47] M. N. ÖZİŞİK. *Boundary Value Problems of Heat Conduction*. Scranton PA: International Textbook Company, 1968.
- [48] S. PHILIPS, E. K. KAO, M. YEE, and C. C. ANDERSON. "Detecting activity-based communities using dynamic membership propagation," in *Proc. IEEE Intl. Conf. Acoustics, Speech and Signal Processing (ICASSP)*, Kyoto, Japan (2012).
- [49] M. A. PINSKY and S. KARLIN. *An Introduction to Stochastic Modeling*. New York: Academic Press (2010).
- [50] A. POTHEN, H. SIMON, and K.-P. LIOU. "Partitioning sparse matrices with eigenvectors of graphs," *SIAM J. Matrix Anal. Appl.* **11**: 430–45 (1990).
- [51] K. K. SABELFELD and N. A. SIMONOV. *Random Walks on Boundaries for Solving PDEs*. Utrecht, The Netherlands: VSP International Science Publishers, 1994.
- [52] M. SAGEMAN. *Understanding Terror Networks*. Philadelphia, PA: U. Pennsylvania Press (2004).
- [53] D. SHAH and T. ZAMAN. "Rumors in a network: Who's the culprit?," *IEEE Trans. Inf. Theory* **57**(8): 5163–5181 (2011).
- [54] D. SHAH. "Gossip Algorithms," *Foundations and Trends in Networking* **3**(1)1–125 (2009).
- [55] A. SHAMIR. "A survey on mesh segmentation techniques," *Computer Graphics Forum* **27**(6): 1539–1556 (2008), Sep. 3 2012 [Online]. Available: (<http://www.faculty.idc.ac.il/arik/site/mesh-segment.asp>).
- [56] S. T. SMITH, A. SILBERFARB, S. PHILIPS, E. K. KAO, and C. C. ANDERSON. "Network Discovery Using Wide-Area Surveillance Data," in *Proc. 14th Intl. Conf. Informat. Fusion (FUSION)*, Chicago, IL (2011).
- [57] S. T. SMITH, S. PHILIPS, and E. K. KAO. "Harmonic space-time threat propagation for graph detection," in *Proc. IEEE Intl. Conf. Acoustics, Speech and Signal Processing (ICASSP)*, Kyoto, Japan (2012).
- [58] S. T. SMITH, K. D. SENNE, S. PHILIPS, E. K. KAO, and G. BERNSTEIN. "Covert Network Detection," *Lincoln Laboratory J.* **20**(1): 47–61 (2013).
- [59] D. A. SPIELMAN and S.-H. TENG. "Nearly-linear time algorithms for graph partitioning, graph sparsification, and solving linear systems," in *Proc. 36th ACM Symp. Theory of Computing (STOC)*, pp. 81–90 (2004).
- [60] D. STIRZAKER. *Stochastic Processes and Models*. Oxford University Press (2005).
- [61] R. TRINQUIER. *Modern Warfare: A French View of Counterinsurgency*. Westport, CT: Praeger Security International (2006).
- [62] P. VAN MIEGHEM, D. STEVANOVIĆ, F. KUIPERS, C. LI, R. VAN DE BOVENKAMP, D. LIU, and H. WANG. "Decreasing the spectral radius of a graph by link removals" *Phys. Rev. E* **84**: 016101 (2011).
- [63] H. L. VAN TREES. *Detection, Estimation, and Modulation Theory*, Part 1. New York: John Wiley and Sons, Inc. (1968).
- [64] U. VON LUXBURG, O. BOUSQUET, and M. BELKIN. "Limits of spectral clustering," in *Advances in Neural Information Processing Systems* **17**, eds. L. K. SAUL, Y. WEISS, and L. BOTTOU. Cambridge, MA: MIT Press (2005).
- [65] S. WASSERMAN and K. FAUST. *Social Network Analysis*. Cambridge University Press. (1994).
- [66] D. J. WATTS. "Networks, dynamics, and the small-world phenomenon," *American Journal of Sociology* **13**(2): 493–527 (1999).
- [67] Y. WEISS. "Segmentation using eigenvectors: A unifying view," in *Proc. of the Intl. Conf. Computer Vision* **2**: 975 (1999).
- [68] S. WHITE and P. SMYTH. "A spectral clustering approach to finding communities in graphs," in *Proc. 5th SIAM Intl. Conf. Data Mining*, eds. H. KARGUPTA, J. SRIVASTAVA, C. KAMATH, and A. GOODMAN. Philadelphia PA, pp. 76–84 (2005).

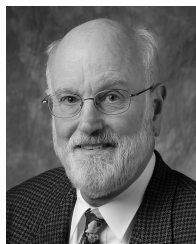
- [69] H. WOLKOWICZ and Q. ZHAO. "Semidefinite programming relaxations for the graph partitioning problem," *Discrete Applied Mathematics* **96–97**: 461–479 (1999).
- [70] J. XU and H. CHEN. "The topology of dark networks," *Comm. ACM* **51**(10): 58–65 (2008).
- [71] M. J. YEE, S. PHILIPS, G. R. CONDON, P. B. JONES, E. K. KAO, S. T. SMITH, C. C. ANDERSON, and F. R. WAUGH. "Network discovery with multi-intelligence sources," *Lincoln Laboratory J.* **20**(1): 31–46 (2013).
- [72] H. ZHOU and R. LIPOWSKY. "Network Brownian Motion: A New Method to Measure Vertex-Vertex Proximity and to Identify Communities and Subcommunities," in *Computational Science—ICCS 2004, Lecture Notes in Computer Science* **3038**: 1062–1069. Berlin: Springer (2004).



Steven Thomas Smith (M'86–SM'04) is a Senior Staff Member at MIT Lincoln Laboratory, Lexington, MA. He received the B.A.Sc. degree in electrical engineering and mathematics from the University of British Columbia, Vancouver, BC in 1986 and the Ph.D. degree in applied mathematics from Harvard University, Cambridge, MA in 1993. He has over 15 years experience as an innovative technology leader with statistical data analytics, both theory and practice, and broad leadership experience ranging from first-of-a-kind algorithm development for groundbreaking sensor systems to graph-based intelligence architectures. His contributions span diverse applications from optimum network detection, geometric optimization, geometric acoustics, statistical resolution limits, and nonlinear parameter estimation. He received the SIAM Outstanding Paper Award in 2001 and the IEEE Signal Processing Society Best Paper Award in 2010. He was associate editor of the *IEEE Transactions on Signal Processing* in 2000–2002, and currently serves on the IEEE Sensor Array and Multichannel committee. He has taught signal processing courses at Harvard and for the IEEE.



Edward K. Kao (M'03) is a Lincoln scholar at MIT Lincoln Laboratory in the Intelligence and Decision Technologies Group. Since joining Lincoln in 2008, he has been working on graph-based intelligence, where actionable intelligence is inferred from interactions and relationships between entities. Applications include wide area surveillance, threat network detection, homeland security, and cyber warfare, etc. In 2011, he entered the Ph.D. program at Harvard Statistics. Current research topics include: causal inference on peer influence effects, statistical models for community membership estimation, information content in network inference, and optimal sampling and experimental design for network inference.



Kenneth D. Senne (S'65–M'72–SM'95–F'02–LF'08) serves as Principal Staff in the ISR and Tactical Systems Division at Lincoln Laboratory. His research examines the application of large data analytics to decision support problems. He joined the Laboratory in 1972 to work on the design and collision avoidance application of the Mode-S beacon system for the Federal Aviation Administration. From 1977 to 1986 he contributed to the development of anti-jam airborne communication systems and super resolution direction finding with adaptive antennas. In 1986 he was asked to set up an array signal processing group as part of a large air defense airborne electronics program. This effort resulted in the pioneering demonstration of a large scale, real-time embedded adaptive signal processor. In 1998 he was promoted to head the Air Defense Technology Division. In 2002 he established the Laboratory's Technology Office, with responsibility for managing technology investments, including the internal innovative research program. Prior to joining Lincoln Laboratory he earned a Ph.D. degree in electrical engineering from Stanford University with foundational research on digital adaptive signal processing and he served as Captain in the U.S. Air Force with the Frank J. Seiler Research Laboratory at the Air Force Academy. He was elected Fellow of the IEEE in 2002.



Garrett Bernstein is a Computer Science Ph.D. student at the University of Massachusetts Amherst. At MIT Lincoln Laboratory, he was a member of the technical staff in the Intelligence and Decision Technologies Group. His research focused on statistical inference and machine learning applied to diverse problems, such as graph detection algorithms, model simulation, semantic analysis, and military operational effectiveness. Prior to joining the Laboratory, he received a bachelor's degree in applied and engineering physics and an engineering master's degree in computer science, both from Cornell University.



Scott Philips is currently a data scientist at Palantir Technologies. Before joining Palantir, Scott spent five years as a member of the technical staff in the Intelligence and Decision Technologies Group. While he was at Lincoln Laboratory, his research focused on developing statistical algorithms for the exploitation of data from intelligence, surveillance, and reconnaissance sensors. Scott received his doctoral degree in electrical engineering in 2007 from the University of Washington, where his research focused on signal processing and machine learning algorithms for the detection and classification of sonar signals.